Paper presented at the 22nd Asian Conference on Remote Sensing, 5 - 9 November 2001, Singapore.

DETERMINATION OF SPATIAL DISTRIBUTION AND FRACTION INDEX OF SMOKE PLUMES GENERATED BY KUWAITI OIL WELL FIRES

Nader Jalali[*], Hamid Taheri[**], Bahram saghafian[*], Bahram Aminipouri[*] and Massoud Tajrishi[***]
Jalali_n@yahoo.com
Fax: ++98 21 4905709

KEY WORDS: NOAA, modelling, smoke plume, Iran

ABSTRACT

Just before the end of the Persian Gulf war in February 1991, more than 700 oil wells in Kuwait were set on fire. Smoke plumes generated from oil well fires affected the Persian Gulf region mandating environmental studies to be undertaken by the countries involved. Several atmospheric and mathematical models were used for modelling the propagation of smoke in the region but, due to lack of sufficient data, these models could not yield reliable results. As an example, the smoke density and movement of smoke plumes were tracked in the region, but less efforts were made to analyse the smoke fractions such as polluttant agents like toxic materials. In this study, the NOAA-AVHRR satellite data were used for tracking and determining smoke fraction patterns. The images marked with smoke were digitally compared with a reference image corresponding to clear atmosphere, in order to measure smoke index. By providing the spatial and temporal pattern of smoke fraction for environmental assessment purposes, the results demonstrated that remote sensing data can be effectively used to track and determine smoke fraction indices for catastrophic past events.

Introduction

Two catastrophic events occurred after the invasion of Kuwait by Iraqi forces on August 2, 1990 (Hosain, 1995). Late January 1991, millions of barrels of crude oil were released into the Persian Gulf from tankers and oil terminals located off coast of Kuwait. Just before the end of the Gulf war in February 1991, more than 700 oil wells in Kuwait oil fields were set on fire (Hosain, 1995). A total of 67 million tons of oil is believed to have burnt (CWRER, 1998). The burning wells in Kuwait produced large amounts of gases as well as particulated matter containing metals and burned hydrocarbon (Hosain, 1995). The amount of soot and sulfur dioxide produced are estimated at 2.0 and 2.1 million tons, respectively (CWRER, 1998).

The resulted smoke plumes traveled mainly down wind over the region. The base of the plume was generally found to be as high as 1 to 2 km above the surface, while the plume top did not exceed 5 km. Contrary to some prewar expectations, due to the lack of considerable vertical wind shear in the region and prevailing inversion due to the difference in temperature above and below the plume, it did not extend into the atmosphere; thus the possibility of a global environmental impact was minimized. Regional and local impacts, however, were severe and significant (CWRER, 1991).

Due to regional and local impacts of air pollution, it is necessary to provide a model to reasonably predict (though for past years) the behavior and spatial-temporal extent of air pollution during 1991. For this purpose, a number of existing mathematical models were reviewed in the second meeting of WMO in 1992, where packages included near-field and regional-global models (WMO, 1992). Yet most of the adopted models failed to generate output satisfactorily comparable to the observed data for soot and gaseous pollutants (Hicks, 1992). Also, most of the models did not consider the diversity of geographical features in the region which will inevitably affect the transportation of the pollutants (WMO, 1992). The effectiveness of some of these models was further hampered due to lack of meteorological and pollution concentration data (Hosain, 1995).

Another group of models are based on processing the satellite data for tracking smoke plumes. Satellite monitoring of the smoke plume during the period of concern verifies the counter-clockwise cyclonic of low pressure over Iran and direct movement of the plume towards the territory of Iran (Vasiliadis & Adib, 1997). According to Limaye et al. (1992) and Cahalan (1992), the sequence of meteosat imagery for May-June 1991 indicated that smoke followed three paths, one of which was direct movement eastward, toward Iran. Limaye et al. (1992) concluded that comparison of satellite observations with winds provided by numerical weather prediction models indicated that most of the smoke was between 850 and 700 mbars.

[*] Soil Conservation and Watershed Management Research Center, P. O. Box 13445-1136, Tehran, Iran
[**] Graduate student of the Civil Engineering Department of Sharif University of Technology.
[***] Assistant Professor of the Civil Engineering Department of Sharif University of Technology.

Aminipouri et al. (1998) produced a model on the basis of processing the NOAA satellite data for tracking the smoke plume in the region. But they didn't consider the effects of the soil moisture, cover class and solar angle in the reference images. Also they didn't create the daily continuous time series of spatial distribution of smoke plume, because of unavailability of daily mid-day local area coverage (LAC) images of NOAA satellite.
In this study, an attempt is made to improve on the model of Aminipouri et al. (1998) by using additional reference image, removing the invalid values and utilizing interpolation methods. Continuous daily time series images showing spatial distribution of smoke plume were also prepared for 21 February to 31 March 1991 period in southwest of Iran.

Region of Study

The study region is located in the Middle-East covering some parts of the countries located around the Persian Gulf (Figure 1). The region boundaries are (44^0,11' to 57^0, 48')E and (21^0, 10' to 33^0, 33')N. The area of this region is approximately 997200 km^2.

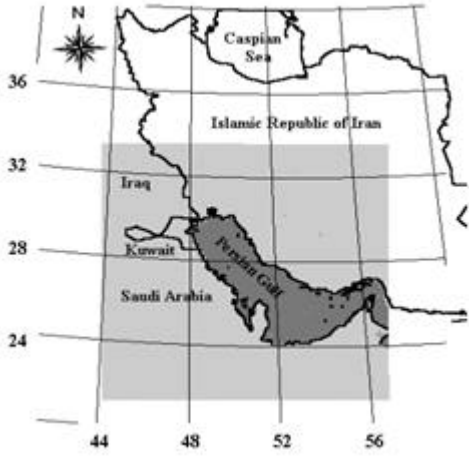

Satellite Imageries used in this study

In this study, mid-day channel2 of GAC* images from the NOAA-AVHRR were used. The reason for choosing the GAC images was lack of good quality LAC** mid-day images within the data set. The spatial resolution of GAC images is approximately 4.0 km. The swath width of NOAA satellite is 2700 km and it covers the entire region of interest (having synoptic view).
Since smoke in channel 2 treats as a good absorber, this channel has been selected as the primary source of data for processing.

Figure 1 : The region of study shown in light gray

Criteria for choosing the mid-day images are:

1. Channel 2(infrared) images have sufficient coming radiation.
2. Shadow and shading effects caused by clouds and mountains should be minimum.

The NOAA-AVHRR images were obtained form National Center for Atmospheric Research (NCAR). The data were read and converted to PC Erdas-Lan format to be processed by ILWIS GIS/image processing package (ITC, 1998). The images were geo-referenced with the boundary of Persian Gulf and other invariant control points.

Proposed Algorithm for Tracking and Determining the Smoke Index

The model proposed in this study is based on the model that was originally presented by Aminipouri et al. (1998). Their model expressed in the following equation is applicable to land areas only:

$$S_f(t) = 1 - \sqrt{\frac{R(t)}{R_{sl}}} \qquad (1)$$

where, R(t) is reflectance in the near infrared channel at time t, R_{sl} is reference value being a function of cover class, relief effect and sun angle for land elements in the "Reference Image", and $S_f(t)$ is the smoke-fraction index at time t. If $S_f(t) < 0$ then the phenomena is cloud or haze, if $S_f = 0$ *the* phenomena is land (no cloud, haze, soot or smoke), and if $S_f(t) > 0$ then the phenomena is smoke or deposited soot. Aminipouri et al. (1998) spent considerable effort on generating LAC reference image form a few available LAC images of May and June 1991.
In this study, the following stages were performed to extract the time series smoke fraction index maps.

* : Global Area Coverage
** : Local Area Coverage

Stage 1: The LAC reference image prepared by Aminipouri et al. (1998) was resampled to GAC resolution and was named R_{SG} (Figure 2).

Stage 2: The model based on Equation 1 was applied on R_{SG} and the channel 2 of GAC mid-day images to produce S_f layers. Figure 3 shows a typical S_f layer corresponding to March 12, 1991.

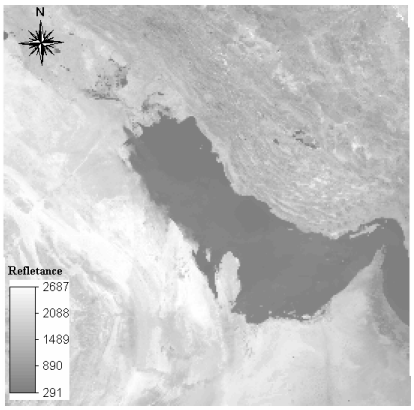

Figure 2: The GAC reference image (R_{SG} image)

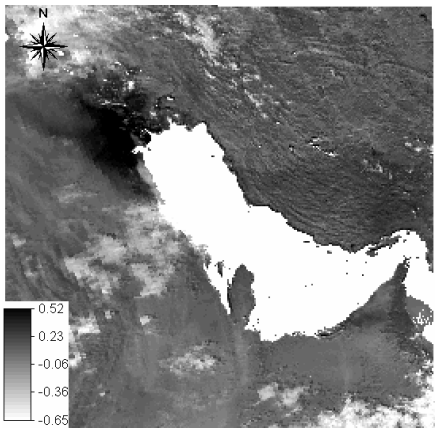

Figure 3:The original smoke fraction index image of 12 March, 1991

Stage 3: By removing the negative values from the S_f layers, the cloud and haze free images were produced. Figure 4 shows the cloud and haze free image of March 12, 1991.

Stage 4: The region of study was almost confined to Iranian territory and the invalid S_f values were removed. The produced images were named $US_f(t)$. Figure 5 shows the US_f corresponding to March 12, 1991.

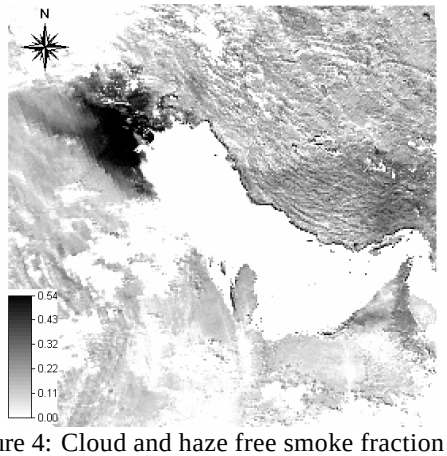

Figure 4: Cloud and haze free smoke fraction index March 12, 1991.(Blank pixels are cloud , haze and water bodies.

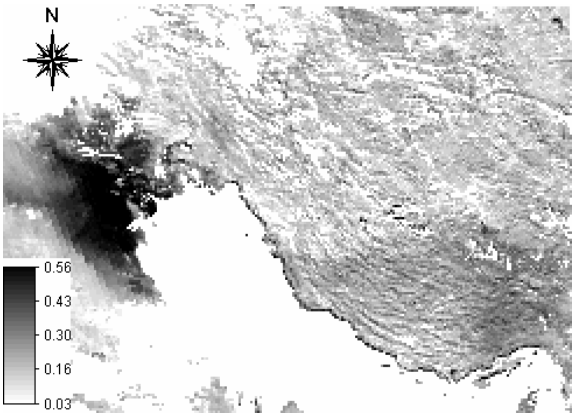

Figure 5: The US_f image of March12,1991

Stage 5: The interpolation operation was performed on the US_f images using inverse distance method to fill for the pixels which have previously had invalid values.

Stage 6: The residual undefined pixels, were filled by Thiessen method. Therefore all the pixels in US_f images were assigned a value. The Persian Gulf area must also be excluded from the region. The images after masking the Persian Gulf are named $Ins_f(t)$. Figure 6 shows the Ins_f image corresponding to March 12, 1991.

Stage 7: Several images prior the Kuwaiti oil well fires were acquired and by applying Equation 1 over these images, clouds, haze and invalid values were removed from them. With combination and averaging of residual

values in those images, one image was produced. In this image, a number of the pixels still remain without value. Using inverse distance interpolation method were assigned to all pixels. This image is named IR_G .

Stage 8: The following equation was applied on IR_G image to produce the new reference image. Equation 2 in fact is the inverse of Equation 1.

$NR_G = R_{SG} \times (1-IR_G)^2$ (2)

where, NR_G is the new reference image.

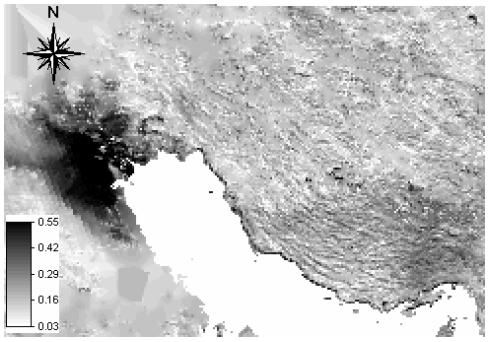

Figure 6: The study area after masking of interpolated US_f image, called "IS_f" for March 12, 1991

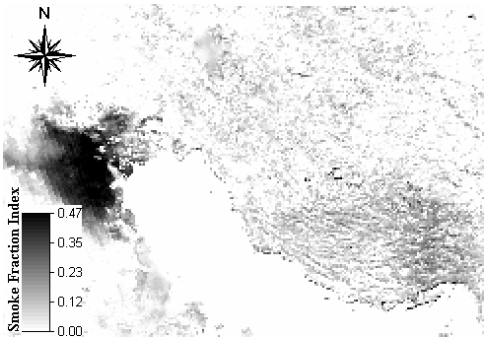

Figure 7: The revised smoke fraction index for March 12, 1991

Stage 9: $RS_f(t)$ images are produced after the application of equation 3 on the $Ins_f(t)$ image.

$RS_f(t) = R_{SG} \times (1-Ins_f(t))^2$ (3)

where, $RS_f(t)$ are the new images where cloud, haze and invalid values have been substituted by land scene values.

Stage 10: $NS_f(t)$ images are produced after the application of Equation 4 on the $RS_f(t)$ images.

$$NS_f(t) = 1 - \sqrt{\frac{RS_f(t)}{NR_G}} \qquad (4)$$

where, $NS_f(t)$ are the smoke fraction index images in which the effects of soil moisture, cover class and sun angle effects has been reasonably incorporated.

Stage 11: With converting the negative values of $NS_f(t)$ images to zero the SFIT (t) images are produced. The SFIT (t) images represent the revised smoke fraction index in the region of study. The Figure 7 shows the SFIT image corresponding to March 12, 1991.

Stage 12: With masking the regions that are out of territory of Iran from SFIT(t) images, the SFI(t) images are produced. The Figure 8 shows the SFI image corresponding to March 12, 1991.

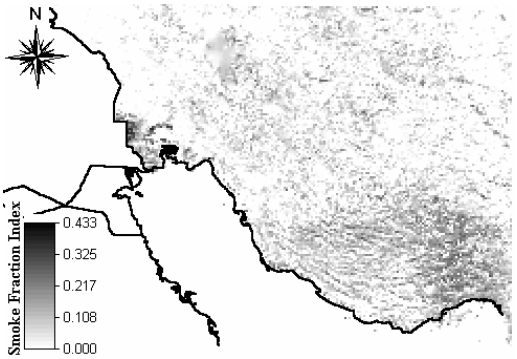

Figure 8: The smoke fraction index (SFI) in the Southwest of Iran in March 12, 1991

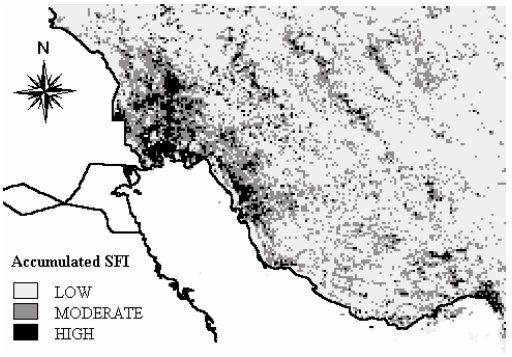

Figure 9: accumulated daily smoke fraction index for February and March, 1991

Discussion

Figure 2 shows the band 2 near infra-red GAC NOAA original reference image. The areas in the South and South-Western parts of the image with high reflectivity correspond to dry desert regions while the area north of the Persian Gulf show less reflectivity likely due to soil moisture and soil cover. The smoke fraction in Figure 3 is based on the original reference image (Figure 2). The areas in Kuwait near the source of well fires are particularly affected by smoke plume which stretches westward due to dominant wind direction on the date of image. Some areas in the South of Iran along the coastline have also been influenced by relatively high smoke fraction. One may see the clouds spread in some part of the image with negative smoke fraction value. If the cloudy areas are removed, the smoke dominated areas may be highlighted as shown in Figure 4. One should expect some degree of error in the resultant smoke fraction images for various days in the months of February and March 1991 since the original reference image was made from two cloud free images of May and June 1990, when moisture, sun angle and vegetation cover are different from those in early months. On the other hand, some pixels in the immediate vicinity of clouds may be affected by cloud, smoke and ground since the spatial resolution is 4 km. Removing such pixels and masking out the Southern part of the smoke fraction layer presented in Figure 5.

The inverse distance interpolation technique was applied to fill the unknown pixels in the smoke fraction layers. The areas outside the limiting distance in large cloud areas were filled using Thiessen polygon method. Figure 6 shows a completed smoke fraction layer corresponding to March 12, 1991.

In order to consider proper season for the reference image, several low-cloudy images prior to the well fires were selected and, after performing stages 7, 8, 9, 10, 11 and 12, the revised smoke index was produced (Figure 8) for the Southwest region of Iran. applying a similar procedure for other images acquired in February and March, generated the time series of smoke fraction layers. As may be seen from these typical maps, the smoke plume occupies different areas following the number and amount of oil wells on fire as well as wind direction.

Summation of smoke fraction maps for February and March as shown in Figure 13 presents the spatial distribution of total smoke index over the territory of Iran. One can identify the coastline areas as the most affected areas in Iran.

Conclusions:

- Remotely sensed data (particularly NOAA-AVHRR) can intensively be used for tracking and monitoring smoke plumes and determination of smoke fraction index in air at regional scale.
- The GAC mid-day images of NOAA-AVHRR are useful sources of information for generating daily smoke fraction index or smoke distribution maps.
- Integration of geographic information systems and image processing techniques could lead to have useful information in a very short time.

References:

Aminipouri, B., Jalali, N, Noroozi, A.A. and Abkar, A.A., 1998. Tracking of oil spills and smoke plumes of Kuwait's oil well fires to the coast and territory of I.R. of Iran as a result of the 1991 Persian Gulf war. Soil Conservation and Watershed Management Research Center of I.R. of Iran, ISBN 90 6164 1489.

Avery, T.E. and Berlin, G.L., 1992. Fundamental of remote sensing and airphoto interpretation. Avery and Berlin.

Cahalan, R.F., 1992. The Kuwait oil fires as seen by Landsat. Journal of Geophys. Res., 97:D13:14565-14571.

CWRER, 1998. Development of a computer based modeling system for the atmospheric air plume movement following Kuwait oil well fires. Center for Water Resources and Environmental Research, The University of New York , New York, USA.

Hicks, B.B., 1992. An overview of the U.S. studies of the Kuwait oil fire plum dispersion. Presented at the Second WMO Meeting of Experts to Assess the Response to the Kuwait oil fires, Geneva, Switzerland, May 25-29.

Hosain, T., 1995. Kuwit oil fires: regional environmental perspectives. 1 st Ed., Elsevier science.

ITC (International Institute for Aerospace survey and Earth science), 1998. GIS and remote sensing software package, ILWIS. Enschede, The Netherlands.

Jalali, N., Aminipouri, B. and Noroozi, A.A., 1999. Tracking of smoke plumes generated by Kuwaiti's oil well fires using model based image analysis. Proceedings of the 5th Asia-pacific Conference on Multilateral Cooperation of Space Technology Applications, I.R. of Iran, Tehran, December 6-9.

Limaye, S.S., Ackerman, S.A., Fry, P.M., Ali, M.I.H., Wright, A. and Rango, A., 1992. Satellite monitoring of smoke from the Kuwait oil fires. Journal of Geophy. Res., 97: D13:14551-14563.

Vasiliadis, H.V. and Adib, F., 1997. Smoke plumes from the 1991 Kuwait oil fires. Center for Water Resources and Environmental Research, The City University of New York, Report No. TR97-CWRER.12.01, December.

WMO, 1992. Report of second WMO meeting of experts to assess the response to and atmospheric effects of Kuwaiti oil fires. Geneva, Switzerland.